Hydrophobe V
5th International Conference on Water Repellent Treatment of Building Materials
Aedificatio Publishers, 31-42 (2008)

X-rays and Neutrons used for the Visualisation of Oligomeric Siloxanes

V. Cnudde[1], B. Masschaele[2], J. Vlassenbroeck[2], M. Dierick[2], Y. De Witte[2], E. Lehmann[3], L. Van Hoorebeke[2] and P. JS. Jacobs[1]
[1]Dept. of Geology and Soil Science, Ghent University, Gent, Belgium
[2]Dept. of Subatomic and Radiation Physics, Ghent University Ghent, Belgium
[3]Department of Spallation Neutron Source, Paul Scherrer Institut, Villigen, CH-5232, Switzerland

Abstract

The study explored the potential of X-rays, as well as that of neutrons, for their use as non-destructive visualisation techniques of oligomeric siloxanes within a natural stone matrix. Contrast in X-ray radiographs depends on the density and atomic number of the materials in question. Although X-ray Computer Tomography (CT) proved to be a very useful technique to examine the internal structure of natural building stones, detecting organic compounds like water repellents within the stone is still very difficult. Neutron CT is based on the same principles as X-ray CT, and its advantages remain underexploited because neutron sources are not as accessible as X-ray ones. Neutrons are particularly suitable in visualising water and non-polymerised water repellents inside stone because of their strong attenuation for hydrogen. As neutrons can quite easily penetrate porous materials such as natural building stone, they can localise water or organic fluids, e.g., hydrocarbons, with high contrast within them. A comparison of the advantages and disadvantages of both techniques is presented. For example, neutron radiography gives a strong contrast between wet and dry regions of partially saturated porous materials as opposed to X-ray tomography that has to make use of contrast agents (like iodine or strong bromine solutions) to detect fluids inside stones.

Keywords: X-ray, neutron, siloxane, stone, porous building materials

1 Introduction

The determination of the localisation of water repellent products inside natural building stones is important to evaluate their effectiveness in conservation. Many direct techniques, such as NMR, microscopy, etc., and indirect measurements, such as capillarity, drying rate, water-vapour permeability determination, etc., are currently used. However, if the exact location of a water repellent inside a porous material is to be determined in three dimensions, this cannot be easily done with these techniques. Therefore a non-destructive 3D technique like computer tomography (CT) was explored. Computer tomography in general – using any kind of penetrating radiation - investigates the external and internal structure of the samples without actually opening or cutting them. Without any form of sample preparation it is possible to obtain a 3D computer model of the sample within a few hours (or less). X-rays, protons and neutrons are some of the possible radiations used for CT. This study focuses on methods using either X-ray or neutron radiation.

X-ray CT is a very common procedure for medical diagnostics and has also been recently applied to material research [1]. The physical parameter, providing the structural information, is the (X-ray) attenuation coefficient μ. This coefficient is the product of the photon mass attenuation coefficient μ/ρ (cm^2/g) and the chemical density ρ (g/cm^3) of the sample. The attenuation coefficient μ depends on the local composition of the sample material. Furthermore, the mass attenuation coefficient depends on the energy of the X-rays: the higher the energy of the photon, the smaller the attenuation in the sample (for energies typically below 200 keV, where the photo-electric effect is the pre-dominant process of interaction). X-ray CT is based on the X-ray transmission information and follows the Lambert-Beer equation (1):

$$I = I_0 \cdot \exp(-\int_L \mu(s) \cdot \rho(s) \cdot ds) \quad (1)$$

with I_o the initial X-ray intensity before passing through the sample, I the intensity after passing through the sample, the linear attenuation coefficient μ(s).ρ(s) of the object being studied and with $\int ds$ the length of the X-ray path through the material (typically a line between the X-ray source and the detector pixel).

As X-ray source for CT, a synchrotron with a parallel, mono-energetic beam or a compact X-ray tube, with a polychromatic cone beam can be used. Synchrotron radiation has the advantage of providing a higher X-ray flux and thus a higher signal-to-noise ratio. An added advantage is the monochromatic nature of the beam, which allows more accurate quantification of the attenuation coefficients and eliminates artefacts like beam hardening. Although synchrotron radiation presents clear advantages over X-ray tube radiation, X-ray tubes are far more available and with significantly lower cost.

X-ray detectors are used to record the attenuation information along lines through the object, according to equation (1). To detect the transmitted X-rays they have to be converted to visible light with scintillation materials like Gadox P43 or CsI crystals. The visible light from the scintillator is in turn registered by CCD cameras, CMOS-flat panels or amorphous Si-flat panels. Direct conversion detectors, like photon counting solid state arrays or amorphous Se, are still not often used but could hold the future for micro-CT.

To perform CT, digital radiographs of the sample are made from different orientations by rotating the sample along the scan axis from 0 to 360 degrees (Fig. 1). A radiograph sums the information of the sample along the rays of the X-ray beam. Radiographs can reveal important information, but in order to obtain a full 3D image of the sample, radiographs derived from different angles need to be acquired.

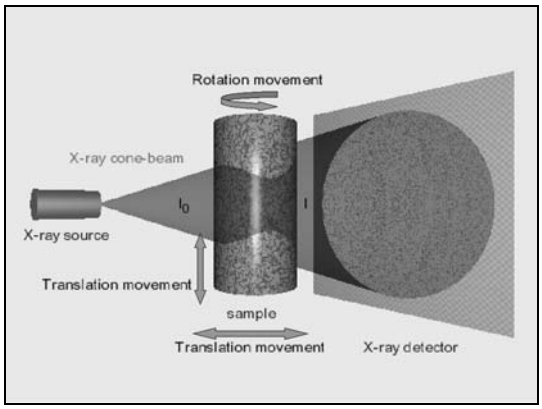

Figure 1: Typical set-up for an X-ray CT system

Theoretically, the number of projections or radiographs necessary to reconstruct the internal structure of the object is the product of the number of horizontal detector pixels and π [2]. This follows from the mathematics behind tomography where in order to have a sufficiently close sampling of the space to be able to reconstruct it the number of pixels has to be multiplied by Pi . In practice, a number of projections roughly equal to the number of pixels in the horizontal direction is sufficient for a good reconstruction. After collecting all the projection data, the reconstruction process is started, which produces horizontal cross-sections of the sample, allowing 3D rendering. Materials such as plastic, wood, polymers with light elements, and even denser objects like sediments and stone, with a much higher attenuation coefficient, can be easily studied with X-rays.

Besides using X-rays, neutrons can be also used for tomography [3]. Neutrons should be particularly suitable to visualise water inside stone because of their strong attenuation for hydrogen, H (mainly by scattering). Because neutrons can quite easily penetrate through materials like natural building stones, they can localise water or organic fluids (such as hydrocarbons) with high contrast [3]. Therefore neutron radiography, and consequently tomography, should be able to document a strong contrast between wet and dry regions of partially saturated porous materials in opposition to X-ray tomography. Neutron radiography is already used to map water-content distributions for a wide range of porous construction materials [4-5], while high-speed neutron tomography is a relatively new imaging technique, used to visualise conservation products inside stone since 2005 [6]. The technique is based on the same principle as X-ray micro-tomography, but uses neutrons instead of X-rays.

2 Methods and materials

2.1 X-ray radiography and tomography

X-ray radiography and tomography experiments were carried out at the Centre for X-ray CT at Ghent University (www.ugct.ugent.be) where a high-resolution X-ray CT system was developed [7]. For this study an X-ray tube FXE-160.50 (dual head open type source from Feinfocus) was used. Since it is an open type, filaments or targets can be easily replaced. From the two tube heads, the transmission type X-ray tube was set at a voltage of 60 kV. No filter besides the aluminum exit window was used. As detector, a remote Rad-eye EV detector (from Rad-icon) was utilised. It is a CMOS sensor with 1024×512 pixels of 48 µm×48 µm. EV stands for extended voltage, which makes the use of the detector possible for tube voltages up to 160 kV.

2.2 Neutron radiography and tomography

The neutron radiography and tomography experiments were carried out at the Neutron Transmission Radiography (NEUTRA) beam line of the SINQ spallation neutron source at PSI (Paul Scherrer Institut, Villigen, Switzerland) [8].

The experiments here described used beam position 2 and 3. Position 2 was used for tomographic experiments and fast radiographs at 9.9 m from the target centre, with a beam diameter of 29 cm, a L/D ratio of 350 and a neutron flux of 7.54 $*10^{6}$ cm^{-2} s^{-1} mA^{-1}. The field of view at this position is 97 mm x 97 mm.

Position 3 was used for the radiographs, the end of the beam line was situated at 13 meters from the SINQ target with L/D at 550. The neutron

flux at this position is $4*10^6$ cm^{-2} s^{-1} mA^{-1}, and has a beam diameter of 40 cm. Position 3 has the highest collimation and the beam diameter enables the best spatial resolution and a large field of view of 279 mm x 279 mm.

The first detector system used was a standard neutron detection system based on a CCD camera that is lens-coupled to a neutron sensitive scintillator, namely a 6LiF/ZnS:Ag screen (ND type) manufactured by Applied Scintillation Technologies. The CCD camera was an Andor DV434 with 1024x1024 pixels of 13 µm each. The pixel size of the scintillator at position 2 is 95 µm, while on position 3 this is 272 µm. For the high speed experiments another detector was used, a custom system developed at NEUTRA based on a Varian PaxScan 2520 flat panel X-ray detector. It was equipped with a 250-mm-thick 6LiF/ZnS:Ag scintillator to make it sensitive to neutrons. This detector is described in detail by Estermann et al. [9].

2.3 Software

In tomography, a set of projections is acquired and reconstructed into a 3D volume, generating a numerical value at every voxel (equivalent to a 'pixel' in two dimensions) which gives an indication of the product of the mass density and X-ray attenuation coefficient at that position. To accomplish this, the software Octopus uses several steps, including pre-processing and reconstruction [10]. Before the actual filtered back-projection can be performed, some corrections have to be made to remove acquisition-specific effects in the data. These corrections comprise flat field and offset image corrections; a thresholded median filter to remove overly bright and dark pixels in the images; a ring filter for the removal of ring artifacts and a correction to compensate tilt of the detector or sample stage in a plane perpendicular to the optical axis of the system. After a final pre-processing step, responsible for the reordering of the projection data to make it suitable for the filtered back-projection algorithm, reconstruction is started. The commercially available software VGStudio MAX v. 1.2.1 (Volume Graphics GmbH, Heidelberg, Germany) was used for 3D volume rendering.

2.4 Natural building stones

Although there is a wide variety of natural building stones, this study focused on two types selected on the basis of their high porosity and their mono-mineral composition. The first is a highly porous bioclastic limestone from Maastricht (Maastrichtian, Upper Cretaceous), while the second one is a quartz arenite of Upper-Landenian age (Palaeocene, Palaeogene), known as the Bray sandstone [3].

Maastricht limestone is a well-sorted, clastic carbonate rock with an average grain size ranging from 0.125 to 0.25 mm, i.e., a calcarenite, with an average porosity of 52 % by volume. It is mainly composed of skeletal components of foraminifera, ostracodes, sponges, bryozoa and

brachiopods, all cemented with some calcite spar. It also contains some glauconite, a small amount of quartz, opaque minerals and some iron oxide. The average pore-size diameter, determined with Mercury Intrusion Porosimetry (MIP), was 39.0µm, ranging from 0.0045µm to 57.7µm, while the average threshold pressure is located at a diameter of 45µm [3].

Bray sandstone mainly consists of quartz grains with varying amounts of iron oxide coating them. Also present are grains of rutile, zircon, opaque minerals and chert. The average grain size of the Bray sandstone is between 0.125 mm and 0.25 mm. Depending on its degree of cementation, the Bray sandstone shows more 'sandy' varieties with a consequent higher porosity, average 17.6 % by volume, and highly cemented 'quartzitic' varieties, with an average porosity of 6.6 % by volume. The pore diameter determined with MIP ranged from 0.0045µm to 25.3µm with an average of 15.7µm and the average threshold pressure is situated between 11µm (for the more quartzitic variety) and 16µm (for the more sandy variety), depending on the degree of cementation.

2.5 Water repellent product

The oligomeric siloxane Hydro10 (10 vol-% in white spirit) (from FTB Restoration) with a small quantity of trifunctional monomers, was selected as a water repellent for these stone materials [3].

The experimental dry weight of Hydro10 is 8.03% and its density before polymerisation is 0.77g/cm³ at 20°C, while after polymerisation, -when the polymer is composed of $[(R)_2$-Si-O-] repeating units-, it increases to 1.07g/cm³. The density was determined by determining the mass and the volume of the product.

3 Results and discussion

3.1 X-ray radiography and tomography

As illustrated in Fig. 2, X-ray CT can provide much information on the internal structure of a stone sample. While Fig. 2A represents a 2D SEM image of the Maastricht limestone, Fig. 2B illustrates a 2D reconstruction of a piece of Maastricht limestone scanned with the high-resolution scanner of UGCT. The pixel- and voxel-size of this scan was 3,23 µm. Compared to SEM research, no sample preparation is required for CT visualisation and more than 400 2D cross-sections can be obtained from 1 scanned sample in a few hours time. Four hundred 2D cross-sections with a separation of 3,23 µm means that the total height of the scanned sample was around 1,3 mm. Fig. 2C illustrates a 3D rendered model of the scanned Maastricht limestone after reconstruction.

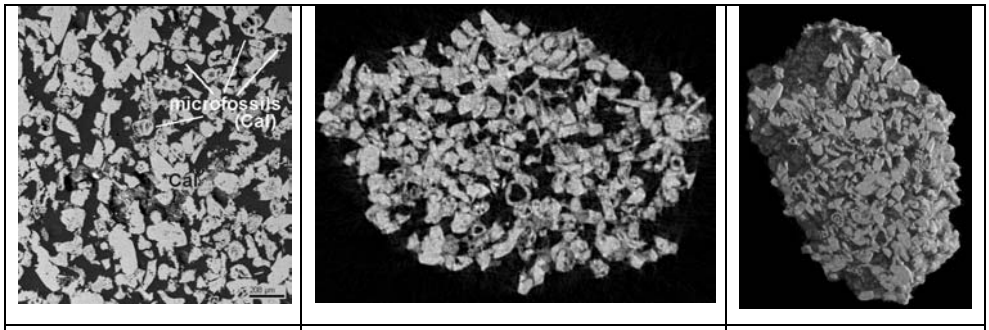

A	B	C

Figure 2: (A) A 2D SEM image of Maastricht limestone, clearly showing the presence of micro-fossils; (B) one of the more then 400 2D reconstructions after CT scan of a Maastricht limestone, also clearly showing the internal structure of the stone; (C) 3D rendered model of the scanned Maastricht limestone

Due to the detail obtained with high-resolution X-ray CT quantification of the samples under investigation is possible. Morpho+, 3D analysis software [10] can provide all kinds of 3D information like porosity, pore-size distribution, shape factors and many more.

For the visualisation of liquids inside natural stone, first an experiment with water in Maastricht limestone was performed. Fig. 3 represents a X-ray radiograph of a sample of Maastricht limestone saturated with water. On this radiograph the water lens, although having a low attenuation for X-rays, can be clearly seen. In order to obtain CT acquisition data, the water should not move during the entire scan, so in order to prevent water evaporation a very fast scanning rate has to be used. The faster the scan is performed, the lower the statistics and the lower the signal-to-noise ratio.

Recording a radiograph or a tomograph means a counting process in which X-ray photons are counted. The accuracy of the measured number of counts is governed by Poisson statistics. Shorter exposure times and/or lower X-ray fluxes lead to lower counts and thus lower accuracy of the measured count values. We call this lower statistics. This is the main noise component in the radiographs. Other noise contributions are electronic noise in the sensor (dark current) and readout noise from the electronics, but these are of lesser importance. All of these make it very difficult to visualise water inside stone during a fast scan.

Figure 3: A radiograph of a Maastricht limestone saturated with water. Note the water lens at the lower left side of the radiograph.

The detection of the polymerised siloxanes inside the stone by means of X-ray micro-CT was already tested by Cnudde in 2005 [3]. Only a clear visualisation of the silicone compounds could be accomplished by doping these products with a material that causes a higher attenuation for X-rays, e.g., 3-bromopropyltrimethoxysilane. By mixing the original water repellent with a higher X-ray attenuation product, higher contrast is obtained allowing their visualisation within the stone material.

When a mixture of 2/3 Hydro10 and 1/3 3-bromopropyltrimethoxysilane was applied by capillary absorption during 5 seconds to a Bray sandstone sample with 13.6% porosity, the presence of the polymerised conservation product could be clearly observed in the reconstructed cross-sections (fig. 4). When the same mixture was applied on cylindrical rock samples with 17% porosity, by means of the spray-flow technique, the polymerised mixture could not be visualized by X-ray CT. Apparently, the amount of product was too low to be detected precisely.

Different factors play a role in the visualisation of the product. The amount of absorbed product, which depends on the porosity and the pore-size distribution of the stone, will influence its visualisation. Furthermore, the concentration of the product into a certain area or its dilution over the entire sample will result in an improved or a reduced visibility of the product, respectively. To obtain a better visualisation, the original products can be doped with a higher amount of 3-bromopropyltrimethoxysilane or with another substance that causes an even higher X-ray attenuation than the 3-bromopropyltrimethoxysilane does. In any case, care should be taken that the doping product should not significantly influence or alter the properties of the original conservation products. In addition, if the amount of highly attenuating product is low and/or the product is homogeneously distributed within the sample as a very thin layer, it is difficult to distinguish the doped product from the stone material. Although these doped products can be visualised with X-ray CT, the fact that a doping agent is needed does not make this technique the most appropriate one since the doping can influence certain characteristics of the original products, even if used in very low amounts.

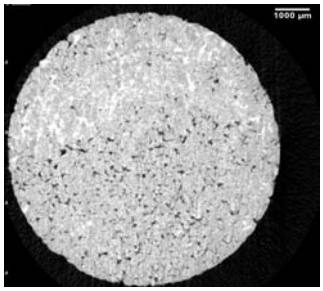

Figure 4: Reconstructed cross-section by X-ray CT of Bray sandstone sample with visualisation of mixture of 2/3 Hydro10 and 1/3 3-bromopropyltrimethoxysilane as bright areas

3.2 Neutron radiography and tomography

Although neutron radiography and tomography have their advantages, they do not allow a detailed 3D quantification of the internal porosity like X-ray CT due to their lower resolution. Fig. 5 presents a neutron radiograph of Maastricht limestone (sample n° 255) treated with a polymerised water repellent (Hydro 10) and an untreated Bray sandstone (sample n°B9). The radiograph shows these samples both in a dry state (top of the figure) and in contact with water (wet state at the bottom of the figure). It can be seen that water (black colour at the bottom of the stones in the bottom part of fig. 5) has a high attenuation for neutrons and the capillary rise of water in the untreated sandstone is clearly visualised [11]. As the Maastricht limestone was treated with a water repellent, no water penetrates into the stone from the bottom.

Previously, Dierick et al. [6] demonstrated that it was also possible to visualise unpolymerised water repellent as it was applied to a natural stone. However, the visualisation of polymerised water repellent by means of neutron radiography or tomography remains a difficult task. Only by looking at the water movement it can be seen that the Maastricht limestone had been treated with a water repellent product.

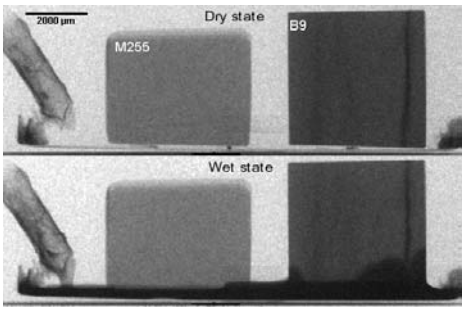

Figure 5: Neutron radiograph of a Maastricht limestone (sample M255) treated with polymerised water repellent Hydro 10 and an untreated Bray sandstone (sample B9) sample in a dry state and in contact with water (wet state)

4 Conclusion

As a non-destructive technique X-ray micro-CT offers the possibility to analyze the internal structure of a natural building stone quickly and at a high resolution. However, the visualisation of oligomer siloxanes inside natural stone remains very difficult. Mixing these water repellent products with highly X-ray attenuating reagents, such as 3-bromo-propyl-trimethoxysilane), may offer a solution.

Alternatively, neutron radiography being particularly sensitive to hydrogen bearing compounds such as water or hydrocarbons, and having a high penetration power, used in neutron tomography complement X-ray tomography in many aspects. In principle, the penetration of fluids in porous materials could be visualised in three dimensions and the distribution of products could be easily assessed during treatment application or soon thereafter. Nevertheless, once water repellent products polymerise they can no longer be visualised by neutron radiography.

Neutron radiography, and consequently tomography documents, show a strong contrast between wet and dry regions of partially saturated porous materials in opposition to X-ray tomographs. These show very poor contrast in the resulting images because of low attenuation for water and the high attenuation for natural building stone. Both X-ray and neutron radiography and tomography have their advantages and disadvantages. Further studies and technical developments are required in order to expand their possibilities.

Acknowledgements

The authors wish to thank the Research Foundation – Flanders for funding the Postdoctoral Fellowships to the first author.

References

[1] V. Cnudde, B. Masschaele, M. Dierick, J. Vlassenbroeck, L. Van Hoorebeke, P. Jacobs. *Recent progress in X-ray CT as a Geosciences Tool*. Applied Geochemistry 21 [5] (2006) 826-832.

[2] A.C. Kak, M. Slaney. *Principles of Computerized Tomographic Imaging*, New York: IEEE Press, 1988.

[3] V. Cnudde. *Exploring the potential of X-ray tomography as a new non-destructive research tool in conservation studies of natural building stones*. Doctoral thesis, Ghent University, 2005.

[4] M. Dawei, Z. Chaozong, G. Zhiping, L. Yisi, A. Fulin, M. Quitian. *The application of neutron radiography to the measurement of water permeability of concrete.* Proceedings of the Second World Conference on Neutron Radiography. Paris, (1986)..255-262.

[5] L. Pel, A.A.J. Ketelaars, O.C.G. Adan, A.A. van Well. *Determination of moisture diffusivity in porous media using scanning neutron radiography*. International Journal of Heat and Mass Transfer 36 (1993) 1261-1267.

[6] M. Dierick, J. Vlassenbroeck, B. Masschaele, V. Cnudde, L. Van Hoorebeke, A., Hillenbach. *High-speed neutron tomography of dynamic processes.* Nuclear instruments & methods in physics research section A: Accelerators, spectrometers, detectors and associated equipment 542 [1-3] (2005) 296-301.

[7] B.C. Masschaele, V. Cnudde, M. Dierick, P. Jacobs, L. Van Hoorebeke, J. Vlassenbroeck. *UGCT: New X-ray radiography and tomography facility*. Nuclear Instruments and Methods in Physics Research Section A: Accelerators, Spectrometers, Detectors and Associated Equipment, 580 [1] (2007) 266-269.

[8] E. Lehmann, P. Vontobel, L. Wiezel. *Properties of the radiography facility NEUTRA at SINQ and its use as European reference facility*. Nondestr. Test. Eval. 16 (2001) 191-202.

[9] M. Estermann, G. Frei, E. Lehmann, P. Vontobel. *The performance of an amorphous silicon flat panel for neutron imaging at the PSI NEUTRA facility*. Nuclear Instruments and Methods in Physics Research A 542 (2005) 253–257.

[10] J. Vlassenbroeck, M. Dierick, B. Masschaele, V. Cnudde, L. Van Hoorebeke, P. Jacobs. *Software tools for quantification of X-ray microtomography at the UGCT*. Nuclear Instruments and Methods in Physics Research Section A: Accelerators, Spectrometers, Detectors and Associated Equipment 580 [1] (2007) 442-445.

[11] V. Cnudde, M. Dierick, J. Vlassenbroeck, B. Masschaele, E. Lehmann, P. Jacobs, L. Van Hoorebeke. *Determination of the impregnation depth of siloxanes and ethylsilicates in porous material by neutron radiography*. Journal of Cultural Heritage 8/4 (2007) 331-338.